

DNA Sequence Evolution with Neighbor-Dependent Mutation

Peter F. Arndt
Department of Physics
UC San Diego
9500 Gilman Drive
La Jolla, CA 92093
arndt@physics.ucsd.edu

Christopher B. Burge
Department of Biology
MIT
77 Massachusetts Ave.
Cambridge, MA 02139
cburge@mit.edu

Terence Hwa
Department of Physics
UC San Diego
9500 Gilman Drive
La Jolla, CA 92093
hwa@matisse.ucsd.edu

ABSTRACT

We introduce a model of DNA sequence evolution which can account for biases in mutation rates that depend on the identity of the neighboring bases. An analytic solution for this class of models is developed by adopting well-known methods of nonlinear dynamics. Results are presented for the CpG-methylation-deamination process which dominates point substitutions in vertebrates. The dinucleotide frequencies generated by the model (using empirically obtained mutation rates) match the overall pattern observed in non-coding DNA. A web-based tool has been constructed to compute single- and dinucleotide frequencies for arbitrary neighbor-dependent mutation rates. Also provided is the backward procedure to infer the mutation rates using maximum likelihood analysis given the observed single- and dinucleotide frequencies. Reasonable estimates of the mutation rates can be obtained very efficiently, using generic non-coding DNA sequences as input, after masking out long homonucleotide subsequences. Our method is much more convenient and versatile to use than the traditional method of deducing mutation rates by counting mutation events in carefully chosen sequences. More generally, our approach provides a more realistic but still tractable description of non-coding genomic DNA, and may be used as a null model for various sequence analysis applications.

Categories and Subject Descriptors

J.3 [Computer Applications]: Life and Medical Sciences—*Biology and Genetics*; G.1.m [Mathematics of Computing]: Numerical Analysis—*Miscellaneous*; I.6.5 [Computing Methodologies]: Simulation and Modeling—*Model Development*; G.3 [Mathematics of Computing]: Probability and Statistics—*Stochastic processes*

General Terms

Algorithms, Measurement, Theory

Permission to make digital or hard copies of all or part of this work for personal or classroom use is granted without fee provided that copies are not made or distributed for profit or commercial advantage and that copies bear this notice and the full citation on the first page. To copy otherwise, to republish, to post on servers or to redistribute to lists, requires prior specific permission and/or a fee.

RECOMB'02, April 18-21, 2002 Washington, D.C., USA
Copyright 2002 ACM 0-58113-498-3-02/04 ...\$5.00

Keywords

CpG-methylation-deamination, DNA sequence evolution, single- and dinucleotide frequencies

1. INTRODUCTION

Models of DNA sequence evolution have generally treated sequences as collections of independently evolving sites[8]. However, there is a substantial amount of evidence from sequence analysis and studies of mutation rates[9] which suggests that the identities of neighboring bases can have a strong influence on the types and rates of mutational events which occur at a given sequence position. We briefly review these types of evidence before describing a model which explicitly accounts for neighbor-dependent mutations.

Biochemical studies in the early 1970s compared the pattern of dinucleotide odds ratios (dinucleotide frequencies normalized for the base composition) or “general designs” of different genomes and different fractions of genomic DNA[17, 18] and concluded that this pattern is a remarkably stable property of a genome which is largely preserved in closely related genomes or in different renaturation rate fractions of the same genome, for example. Some two decades later, a significant body of sequence analysis work primarily by Karlin and coworkers[10, 11, 12] has elaborated and expanded on these observations, showing that the pattern of dinucleotide relative abundance values (essentially equivalent to the general design) constitutes a “genomic signature” in the sense that it is remarkably constant across different parts of a genome and is generally similar between related organisms, but quite different between distantly related organisms. This latter finding has led to application of this principle to phylogeny reconstruction and identification of laterally transferred genes in both prokaryotic and eukaryotic organisms. Although quite promising, this line of work is open to the criticism that there is no underlying theory for why a genome should possess a particular signature or the mechanism by which signatures change over long periods of time. The model described here may help to provide a theoretical framework for interpreting these and related observations. Our analysis may also contribute to understanding of the mechanisms of DNA mutation and repair and may help in the development of better methods for phylogenetic tree construction.

Possible factors relating to the genome signature include effects related to DNA structure, base stacking and thermodynamics as well as a variety of mutational factors. Since the genome signature is particularly pronounced in non-coding sequences which are typically under much less selective pressure than coding regions and evolve much more rapidly, it appears likely that “nonselective” forces such as biases related to mutation, replication and DNA repair account for many of the properties of the genome signature, especially in higher eukaryotic organisms with large genomes containing mostly non-coding DNA and relatively small effective population sizes. One of the most common types of mutation in vertebrate genomes is CpG methylation followed by deamination and mutation of CG/CG to TG/CA [4, 16]. For example, Wang *et al.*[20] found that single-nucleotide polymorphisms occur approximately tenfold more often at CpG dinucleotides than at other dinucleotides in human genomic DNA, suggesting that this is by far the most common type of single base mutation in humans. This is in agreement with the earlier finding by Batzer *et al.*[2] and Hess *et al.*[9] that point substitutions occur 10 times more frequently at CpG sites compared to non-CpG sites. Increased mutation rate associated with CpG methylation can explain at least qualitatively why CpG dinucleotides have consistently extremely low relative abundance values in all vertebrate nuclear genomes[11]. This effect was recently exploited by Fryxell and Zuckerkandl[5] in their theory of the origin of genomic isochores in mammals.

Here we consider a model for DNA sequence evolution which includes neighbor-dependent mutation effects. Efficient computational tools are constructed to solve the model for arbitrary user-specified mutation processes and rates. The main results are quantitative answers to (1) the long term effects of neighbor-dependent mutations on the base compositional structure of a genome, and (2) the underlying mutation processes and rates given sequence data with dinucleotide correlations. In principle, such a model should be able to account for the effects of CpG-methylation induced mutation and several other known contextual effects on mutation rates. However, in order to preserve the tractability of the model, certain other types of mutations which occur in nature had to be ignored. For example mutations which change the lengths of DNA sequences (insertions and deletions such as those caused by polymerase slippage) or more complex mutations such as inversions or other large-scale rearrangements are not considered. Nevertheless, the current model is a reasonable first approximation to DNA sequence evolution in the absence of selection.

This paper is organized as follows: In Sec. 2, we introduce our model of sequence evolution with neighbor-dependent mutation, and define the mutation rate matrices. In Sec. 3, we describe the general scheme used to calculate the single and dinucleotide frequencies, and present the pattern of dinucleotide odds ratio obtained for a particular example involving the CpG-methylation-deamination process described above. We also present the backward analysis, where a maximum likelihood approach is used to *infer* the mutation rates from the observed dinucleotide frequencies within the confines of our model. A web server is made available for the public to perform these calculations at <http://bioinfo.ucsd.edu/dinucleotides>. In Sec. 4, we

list some of a large number of studies made possible by the method described here. Details of the method are relegated to the Appendix.

2. THE MODEL

We consider a sequence of L nucleotides $\alpha_1, \alpha_2, \dots, \alpha_L$ with $\alpha_i \in \{\mathbf{A}, \mathbf{C}, \mathbf{G}, \mathbf{T}\}$. The configuration at time t is denoted by $\vec{\alpha}(t) = (\alpha_1(t), \alpha_2(t), \dots, \alpha_L(t))$. There are two types of mutation processes allowed: (1) mutations of a single nucleotide $\alpha_i \rightarrow \alpha'_i$ which occurs with a rate $Q_{\alpha\alpha'}$ independent of its neighbors, and (2) mutations of a pair of neighboring nucleotides $\alpha_i\alpha_{i+1} \rightarrow \alpha'_i\alpha'_{i+1}$ which occurs with a rate $R_{\alpha\beta\alpha'\beta'}$. These rates are positive numbers and fixed in time.

We start with an initial random sequence $\vec{\alpha}(0)$. The dynamics of the model is Markovian. At any time t , the sequence $\vec{\alpha}(t)$ is updated in discrete time steps $\Delta t/L$ according to the following update rules:

1. A position i is chosen at random between 1 and L ;
2. The nucleotide α_i from the sequence $\vec{\alpha}(t)$ is mutated to α'_i with

$$\Pr(\alpha'_i|\alpha_i) = \begin{cases} 1 + Q_{\alpha_i\alpha'_i} \cdot \Delta t & \text{for } \alpha_i = \alpha'_i \\ Q_{\alpha_i\alpha'_i} \cdot \Delta t & \text{otherwise} \end{cases} \quad (1)$$

to generate an intermediary sequence $\vec{\alpha}'(t)$;

3. A pair of neighboring positions j and $j+1$ is chosen at random between 1 and L ;
4. The nucleotides $\alpha'_j\alpha'_{j+1}$ from the sequence $\vec{\alpha}'(t)$ are mutated to $\alpha''_j\alpha''_{j+1}$ with

$$\Pr(\alpha''_j\alpha''_{j+1}|\alpha'_j\alpha'_{j+1}) = \begin{cases} 1 + R_{\alpha'_j\alpha'_{j+1}\alpha''_j\alpha''_{j+1}} \cdot \Delta t & \text{for } \alpha'_j = \alpha''_j \text{ and } \alpha'_{j+1} = \alpha''_{j+1} \\ R_{\alpha'_j\alpha'_{j+1}\alpha''_j\alpha''_{j+1}} \cdot \Delta t & \text{otherwise} \end{cases} \quad (2)$$

to generate the new sequence $\vec{\alpha}(t + \Delta t/L)$.

To guarantee the conservation of the transition probabilities, the rates must be chosen such that $Q_{\alpha\alpha} = -\sum_{\alpha'} Q_{\alpha\alpha'}$ and $R_{\alpha\beta\alpha\beta} = -\sum_{\alpha'\beta'} R_{\alpha\beta\alpha'\beta'}$. The time increment Δt should be chosen such that all non-diagonal transition probabilities in Eqs. (1) and (2) are small ($\ll 1$). Then after L such iterations, on average every base in the sequence $\vec{\alpha}(t)$ is mutated with probability $(Q + R) \cdot \Delta t$, corresponding to a net increment of time by Δt . The above procedure is then repeated for a long time¹ until the *stationary state* is reached. Since the model is ergodic, the stationary state is unique. We denote the probability to find a configuration $\vec{\alpha}$ in the stationary state by $P(\vec{\alpha})$.

We refer to rates $Q_{\alpha\alpha'}$ and $R_{\alpha\beta\alpha'\beta'}$ collectively as the mutation matrix \mathbf{Q} and \mathbf{R} , respectively. There are a total of 12 independent rates $Q_{\alpha\alpha'}$ and 240 independent rates $R_{\alpha\beta\alpha'\beta'}$. Note that in the special case of neighbor-dependent single nucleotide mutation, e.g., the CpG-methylation-deamination

¹Dynamical aspects of this evolution model will be discussed elsewhere[1].

process described in Sec. 1, \mathbf{R} is given by a *restricted* form with $R_{\alpha\beta\alpha'\beta'}$ non-zero only if $\alpha = \alpha'$ or $\beta = \beta'$. There are still 96 independent rates under this restriction. For non-coding DNA sequences, mutations on the complementary DNA strand should generally occur at the same rate as on the forward strand. We therefore expect a *reverse complementary symmetry* in the rates, i.e., $Q_{\alpha\beta} = Q_{\bar{\alpha}\bar{\beta}}$, and $R_{\alpha\beta\gamma\delta} = R_{\bar{\beta}\bar{\alpha}\bar{\delta}\bar{\gamma}}$, where $\bar{\alpha}$ denotes the complement of α , e.g. $\bar{A} = T$. These complementarity conditions reduce the number of independent parameters by another factor of two. Note however that for the calculation to be presented below, it is not necessary to impose any of these conditions on \mathbf{Q} or \mathbf{R} .

3. METHODS AND RESULTS

The subject of this study is the stationary probability distribution $P(\vec{\alpha})$ for the mutation processes characterized by the rates \mathbf{Q} and \mathbf{R} . If each nucleotide position evolves independently of each other, i.e., if $\mathbf{R} = 0$, then the distribution factorizes, with $P(\vec{\alpha}) = \prod_i P_0(\alpha_i)$, where $P_0(\alpha)$ is given by the eigenvector corresponding to the largest eigenvalue of \mathbf{Q} . However, for $\mathbf{R} \neq 0$, the bases in the sequence do not evolve independently and the stationary distribution is difficult to calculate. Instead, we focus on the single nucleotide frequencies (or the ‘‘base composition’’) and the dinucleotide frequencies, given by

$$f_{\alpha} \equiv \frac{1}{L} \sum_{i=1}^L \sum_{\beta} \delta_{\beta_i\alpha} P(\vec{\beta}) \quad (3)$$

$$f_{\alpha\beta} \equiv \frac{1}{L-1} \sum_{i=1}^{L-1} \sum_{\vec{\gamma}} \delta_{\gamma_i\alpha} \delta_{\gamma_{i+1}\beta} P(\vec{\gamma}), \quad (4)$$

respectively. An important motivation for computing these frequencies is that they are easily measured from actual sequence data[10] and can thus be used for quantitative comparison with the output of our model.

3.1 Forward analysis: Computation of nucleotide frequencies

Our first goal is to compute the frequencies f_{α} and $f_{\alpha\beta}$ in the stationary state for any set of mutation rates \mathbf{Q} and \mathbf{R} . Exact solution of these quantities is still difficult because in order to compute the dinucleotide frequencies, one needs to know the trinucleotide frequencies $f_{\alpha\beta\gamma}$, etc., ending up with an infinite hierarchy of equations. This is a frequently encountered problem in coupled dynamical systems. Here we introduce an approximation procedure called the ‘‘two-cluster approximation’’ which is well-known from nonlinear dynamics[3]. This procedure truncates the hierarchy of equations, expressing the trinucleotide frequencies as a function of the single and dinucleotide frequencies, i.e.,

$$f_{\alpha\beta\gamma} = f_{\alpha\beta} f_{\beta\gamma} / f_{\beta}, \quad (5)$$

and then solves for the dinucleotide frequencies simultaneously. The procedure gives the exact solution if the stationary state of the mutation process \mathbf{R} is a first-order Markov chain; it is generally very accurately as long as the sequence correlation in the stationary state is short-ranged. Comparison of solutions obtained using this method with the best

numerical estimate from Monte-Carlo simulation yielded relative disagreement well below the 1% level; see below. Thus, for practical purposes, we can regard the cluster approximation as generating ‘‘exact’’ results. The advantage of using the cluster approximation (instead of Monte-Carlo simulation) is that the single and dinucleotide frequencies can be computed virtually instantaneously by numerically solving a set of algebraic equations for *arbitrary* mutation matrices \mathbf{Q} and \mathbf{R} , i.e., without any constraints on the rates. We have developed a web server at <http://bioinfo.ucsd.edu/dinucleotides> to perform this calculation.

We will present our method here via a specific example, the CpG-methylation-deamination process described in the introduction. This process is described by a single neighbor-dependent mutation rate, i.e.

$$R_{CGCA} = R_{CGTG} = r \quad (6)$$

and $R_{\alpha\beta\gamma\delta} = 0$ for all other nondiagonal entries. To make this example transparent, we also consider a simplified version of the neighbor-independent mutation rate \mathbf{Q} , adopting a single rate q for all transitions and another rate p for all transversions, i.e.,

$$Q_{AG} = Q_{GA} = Q_{CT} = Q_{TC} = q, \quad (7)$$

$$Q_{AC} = Q_{CA} = Q_{AT} = Q_{TA} = Q_{CG} = Q_{GC} = Q_{GT} = Q_{TG} = p. \quad (8)$$

For this simple case, the single and dinucleotide frequencies can be solved analytically in *closed form* under the two-cluster approximation as described in the Appendix. Note that since the stationary state does not involve any time scale in itself, the results only depend on two effective parameters, q/p and r/p . The transition/transversion ratio has been estimated to be $q/p \approx 3$ previously, based on mammalian pseudogene studies[7, 9, 13, 21]. Combined with the observed 10-fold difference[2, 9] in point substitution counts between CpG and non-CpG sites [which implies $2(r+q) \approx 10 \times (2p+q)$], we obtain $r/q \approx 20$ for mammals. The nucleotide frequencies computed according to these rates are shown in Table 1. They compare very well to the results of Monte-Carlo simulation: the latter performed for an $L = 10^8$ system (and averaged over 100 simulations) yielded results that were within an rms deviation of 10^{-5} in the single-nucleotide frequencies and $4 \cdot 10^{-5}$ in the dinucleotide frequencies.

α	f_{α}	$f_{\alpha A}$	$f_{\alpha C}$	$f_{\alpha G}$	$f_{\alpha T}$
A	0.28606	0.07475	0.06119	0.06827	0.08182
C	0.21394	0.08052	0.05071	0.01442	0.06827
G	0.21394	0.05625	0.04577	0.05071	0.06119
T	0.28606	0.07451	0.05625	0.08052	0.07475

Table 1: Single and dinucleotide frequencies from the two-cluster approximation for $q/p = 3$ and $r/p = 20$.

Let us examine the results presented in Table 1. First we note that the nucleotide composition f_{α} is skewed towards A and T, with a C+G content of 42%, which is in general agreement with the typical average C+G content in mammals. Note that unlike most existing phylogenetic studies[8], where the mutation rates \mathbf{Q} are *tuned* to reproduce the ob-

served frequencies. In our study, the mutation matrix \mathbf{Q} by itself would have generated equal C+G and A+T content, with the anomaly coming solely from the CpG-methylation-deamination process. Similar observation was made in [5] based on Monte Carlo simulations.

Next, we analyze the dinucleotide frequencies. It is useful to focus on the dinucleotide *odds ratio*, $\rho_{\alpha\beta} \equiv f_{\alpha\beta}/(f_{\alpha}f_{\beta})$, introduced to indicate whether a specific dinucleotide pair $\alpha\beta$ is over- ($\rho_{\alpha\beta} > 1$) or under-represented ($\rho_{\alpha\beta} < 1$) with respect to neighbor-independent mutation. The results derived from the frequencies in Tables 1 are shown in Table 2 (top). For comparison, the odds ratio $\hat{\rho}_{\alpha\beta}$ obtained from the *observed* single and dinucleotide frequencies \hat{f}_{α} and $\hat{f}_{\alpha\beta}$ for a region of 4Mbp intergenic DNA taken from the Human genome Chromosome 21 (Accession # NT 011512) is given in Table 2 (bottom). [We will denote each observed quantity by a “hat” throughout the text.] The rms deviation between the observed ratio $\hat{\rho}_{\alpha\beta}$ and the computed $\rho_{\alpha\beta}$ ’s is 0.1. We note that the computed ratios capture correctly the key feature of the observed data, i.e., a strong under-representation of the CG dinucleotides, compensated by the over-representation of CA and TG.

$\rho_{\alpha\beta}$	$\beta = \text{A}$	C	G	T
$\alpha = \text{A}$	0.91	1.00	1.12	1.00
C	1.32	1.11	0.32	1.12
G	0.92	1.00	1.11	1.00
T	0.91	0.92	1.32	0.91

$\hat{\rho}_{\alpha\beta}$	$\beta = \text{A}$	C	G	T
$\alpha = \text{A}$	1.10	0.87	1.11	0.91
C	1.20	1.21	0.20	1.11
G	0.99	1.05	1.22	0.87
T	0.80	0.99	1.21	1.10

Table 2: Top: Dinucleotide odds ratios of the model based on the single and dinucleotide frequencies in Table 1. Bottom: odds ratios obtained for a region of 4Mbp intergenic DNA taken from the Human genome Chromosome 21 (Accession # NT 011512).

At this stage of the analysis, we cannot expect a perfect match between the observed and the computed frequencies in Table 2, since we used a very rough estimate on the rates q and r in the computation. One can of course always tune q and r to match the computed odds ratios in CG and CA/TG. But this is not sufficient for deducing the underlying mutation rates, since the CpG mutation process introduced also affects the other dinucleotide counts: As seen in Table 2 (top), our model produces 9 other dinucleotides that are over- or under-represented by $\sim 10\%$ each. They result from secondary mutation since all these 9 pairs are only *one* point mutation away from CG, CA, or TG. Only the four dinucleotides (AC, AT, GC, GT) that are *two* point mutations away are not affected by the CpG process. Note that the magnitude of the change in $\rho_{\alpha\beta}$ due to the primary mutation, as well as the magnitude and sign of change in $\rho_{\alpha\beta}$ due to the secondary mutations could not have been anticipated directly from the model defined by Eqs. (6)–(8). Thus, the “backward analysis” of matching *all* of the dinucleotide ratios (as well as the single nucleotide frequencies) by varying the rates q and r is a highly nontrivial numerical task. Fryxell and

Zuckerandl[5] attempted to do this by focusing on a few selected nucleotide frequencies (namely, CG, TG, TA and AT) which they obtained for different mutation rates using extensive Monte Carlo simulation. Their method is arbitrary, inaccurate and very time consuming. With our approach, we can provide a systematic, accurate, and efficient method to perform the backward analysis as described below. Our method is implemented in a server at the same url as provided above, <http://bioinfo.ucsd.edu/dinucleotides>.

3.2 Backward analysis: Estimation of mutation rates

Our next task is to estimate the mutation rates \mathbf{Q} and \mathbf{R} which best “explain” the observed data as quantified by single and dinucleotide frequencies \hat{f}_{α} and $\hat{f}_{\alpha\beta}$. We will adopt the strategy of maximum likelihood[14]. Specifically, we compute the likelihood $\mathcal{L}(\mathbf{Q}, \mathbf{R})$ of observing the data given our mutation model with the rates \mathbf{Q} and \mathbf{R} : First we note that the probability $P(\vec{\alpha})$ of observing a sequence $\vec{\alpha}$ of length L is

$$P(\vec{\alpha}) = f_{\alpha_1 \dots \alpha_L} \approx \prod_{i=2}^L (f_{\alpha_{i-1} \alpha_i} / f_{\alpha_i})$$

according to the two-cluster approximation (see Eq. (5) and the Appendix). The likelihood of the occurrence of a particular sequence with frequencies \hat{f}_{α} and $\hat{f}_{\alpha\beta}$ is then given by $(\prod_{\alpha\beta} \hat{f}_{\alpha\beta}^{L \hat{f}_{\alpha\beta}}) / (\prod_{\alpha} \hat{f}_{\alpha}^{L \hat{f}_{\alpha}})$ yielding the following expression for the log-likelihood,

$$\log \mathcal{L} = L \sum_{\alpha\beta} \hat{f}_{\alpha\beta} \log(f_{\alpha\beta}) - L \sum_{\alpha} \hat{f}_{\alpha} \log(f_{\alpha}), \quad (9)$$

where f_{α} and $f_{\alpha\beta}$ denote the single- and dinucleotide frequencies according to our model with rates \mathbf{Q} and \mathbf{R} .

In principle, one can now search through all of the single-point mutation rates as embodied in \mathbf{Q} and all possible combinations of the neighbor-dependent mutation processes and their rates as embodied in \mathbf{R} to maximize \mathcal{L} . However, this search space is much too large even given our solution. More importantly, we do not want to have too many parameters to over-fit the data. Thus, we allow only a single transversion rate (which is set to 1 without loss of generality), two transition rates, $Q_{AG} = Q_{TC}$ and $Q_{CT} = Q_{GA}$ (since a difference in those rates has already been reported in the literature[15]), and one single neighbor-dependent mutation process. However, we do not limit the latter to CpG and search through all of the 48 possibilities and their accompanying rates. If the maximum-likelihood solution found is still not satisfactory, then an additional neighbor-dependent process may be included to further improve the result.

To illustrate the backward analysis, we feed in the single and dinucleotide counts of the above mentioned intergenic region of Human Chromosome 21. The best neighbor-dependent process found by our program is the known process CpG \rightarrow CpA or CpG \rightarrow TpG. However, the transition rates corresponding to the maximum likelihood solution are at the boundary of the region searched. They are even smaller than the transversion rate $p = 1$, indicating that there is something wrong, most likely a sign that the data contained some feature(s) not anticipated by our mutation model. In

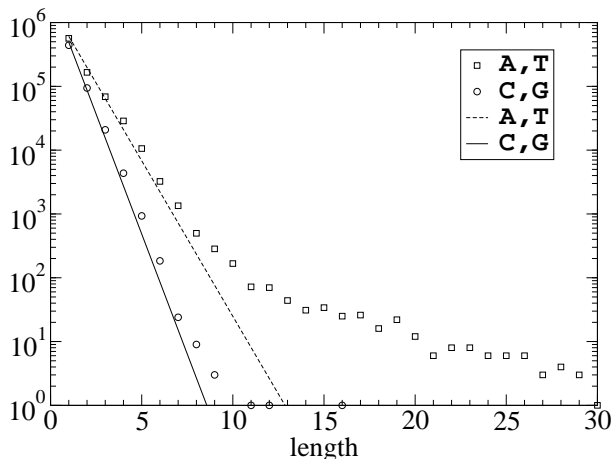


Figure 1: The number of homonucleotide subsequences of a given length in the above mentioned sample of 4Mbp intergenic DNA taken from the Human Chromosome 21. The straight lines represent the expected distributions of such subsequences according to their observed single-nucleotide frequencies of bases and assuming no correlations between neighboring bases.

order to get a hint at the source of the problem, we repeated the search allowing for an additional neighbor-dependent mutation process which would bring the transition rates to the expected regime. The program found the additional processes $\text{ApC} \rightarrow \text{ApA}$ or $\text{GpT} \rightarrow \text{TpT}$; with these processes, the maximum-likelihood solution for the mutation rates became more reasonable, with $Q_{\text{AG}} = Q_{\text{TC}} = 3.10p$, $Q_{\text{CT}} = Q_{\text{GA}} = 3.78p$, $R_{\text{CGCA}} = R_{\text{CGTG}} = 43.02p$, and $R_{\text{ACAA}} = R_{\text{GTTT}} = 4.35p$. Since we are not aware of any biological or biochemical evidence for the additional mutation processes $\text{ApC} \rightarrow \text{ApA}$ or $\text{GpT} \rightarrow \text{TpT}$, we interpret this result merely as an indication that the over-abundance of AA and TT in the observed data (see Table 2) makes it difficult to “explain” by the model with only the CpG mutation process. (From the top panel of Table 2, it is clear that the CpG process only *reduces* the odds ratio of AA and TT , while the observed trend is the opposite.)

What might be the source of this over-abundance? From an inspection of the length distribution of the homonucleotide subsequences (Fig. 1), one sees an conspicuous over-abundance of long runs of A’s or T’s. These long runs, while low in numbers, will clearly bias the dinucleotide counts. However, their occurrences are thought to arise from sequence-specific insertion processes such as polymerase slippage and have nothing to do with neighbor-dependent mutation being studied here. In order to perform the backward analysis properly, it is therefore necessary to first *filter out* the effect of such processes. The odds ratio $\hat{\rho}_{\alpha\beta}^{(\text{filter})}$ obtained after removing all homonucleotide subsequences of length four or more are presented in Table 3 (top). Comparing it to Table 2 (bottom), we see substantial ($> 15\%$) decreases in the counts for AA , TT , CC , and GG as expected, as well as $> 10\%$ increases in AT and TA . (The single nucleotide frequencies are however not affected much by the filter.) Applying the backward analysis on the filtered data with a single neighbor-dependent process, we recover the known CpG process a-

gain, but this time with the rates $Q_{\text{AG}} = Q_{\text{TC}} = 1.75p$, $Q_{\text{CT}} = Q_{\text{GA}} = 2.33p$, and $R_{\text{CGCA}} = R_{\text{CGTG}} = 22.17p$, which are all within the known range given above. [Similar results were obtained when we filtered out subsequences of length 5 or longer with at least 80% of the same nucleotide. The rates found were $Q_{\text{AG}} = Q_{\text{TC}} = 1.66p$, $Q_{\text{CT}} = Q_{\text{GA}} = 2.03p$, and $R_{\text{CGCA}} = R_{\text{CGTG}} = 17.80p$.] The predicted odds ratio ρ^* corresponding to these maximum-likelihood rates are presented in Table 3 (bottom). The rms deviation between the filtered data and the maximum-likelihood prediction is 0.05.

$\hat{\rho}_{\alpha\beta}^{(\text{filter})}$	$\beta = \text{A}$	C	G	T
$\alpha = \text{A}$	0.91	0.92	1.18	1.02
C	1.26	1.05	0.23	1.18
G	1.02	1.02	1.05	0.92
T	0.90	1.02	1.26	0.91

$\rho_{\alpha\beta}^*$	$\beta = \text{A}$	C	G	T
$\alpha = \text{A}$	0.93	1.00	1.11	1.00
C	1.30	1.09	0.24	1.11
G	0.94	1.00	1.09	1.00
T	0.91	0.94	1.30	0.93

Table 3: Top: Observed dinucleotide odds ratios of intergenic DNA taken from the Human genome Chromosome 21 (Accession # NT 011512) with all homonucleotide subsequences of four or more bases filtered out. Bottom: The odds ratio ρ^* corresponding to the maximum-likelihood solution of the backward analysis. The rms deviation between the two odds ratios is 0.05.

4. DISCUSSION AND OUTLOOK

We have introduced a model of neighbor-dependent mutation and developed methods to study these processes which are believed to play an important role in the evolution of genomic sequences. We see that the base composition and the dinucleotide frequencies are strongly influenced by neighbor-dependent mutation. This may contribute to the (surprising) success of phylogenetic analysis based on dinucleotide counts[11, 12], since the pattern of dinucleotide frequencies reflect the mutation mechanisms and rates which should be highly conserved throughout evolution. A similar mutation model was investigated in Ref. [5] using Monte Carlo simulations. In that work, the backward analysis required a number arbitrary assumptions and large amounts of computer time. Our work represents a systematic approach to these studies. The analysis tools we provide enable the users to examine a large number of mutation processes and rates in detail and over a large number of genomes, to look for previously unknown mutation processes and track them across the different kingdoms of life.

Of course, the mutation model (i.e., Eqs. (1) and (2)) and the assumption of stationarity for observed sequences need to be verified quantitatively. But the present method is in fact not limited to the study of the stationary state, and can be straightforwardly extended to describe the evolution towards stationarity[1]. This can be used to extend the traditional phylogenetic analysis[8] to include neighbor-dependent effects, and should be particularly useful for the vertebrates which are dominated by the CpG -methylation-

deamination process. Finally we note that a more accurate description of the evolution of non-coding genomic DNA sequences will be of value to various sequence analysis applications, particularly those involving mammalian genomes. For instance, in the comparative genomics approach to gene and DNA motif finding, one needs to evaluate the probability of spurious matches due to shared common ancestry in the non-coding regions[19]. Accurate evaluation of such probabilities depend critically on having realistic models of sequence evolution, which this study contributes towards.

5. ACKNOWLEDGMENT

The authors are grateful to the hospitality of the Institute for Theoretical Physics (Santa Barbara) where this work was initiated. PFA and TH are supported by the NSF through grant DMR-9971456. PFA additionally acknowledges the financial support by a DFG fellowship, and CBB and TH by functional genomics innovation awards from the Burroughs Wellcome Fund.

6. REFERENCES

- [1] P. F. Arndt and T. Hwa. *in preparation*.
- [2] M. A. Batzer, G. E. Kilroy, P. E. Richard, T. H. Shaikh, T. D. Desselte, C. L. H. CL, and P. L. Deininger. Structure and variability of recently inserted alu family members. *Nucleic Acids Res.*, 18:6793, 1990.
- [3] D. ben Avraham and J. Köhler. Mean-field (n,m)-cluster approximation for lattice models. *Physical Review A*, 45:8358, 1992.
- [4] C. Coulondre, J. H. Miller, P. J. Farabaugh, and W. Gilbert. Molecular basis of base substitution hotspots in e. coli. *Nature*, 274:775, 1978.
- [5] K. J. Fryxell and E. Zuckerkandl. Cytosine deamination plays a primary role in the evolution of mammalian isochores. *Mol. Biol. Evol.*, 17:1371, 2000.
- [6] C. W. Gardiner. *Handbook of Stochastic Methods*. Springer, New York, 1996.
- [7] T. Gojobori, W.-H. Li, and D. Graur. Patterns of nucleotide substitution in pseudogenes and functional genes. *J. Mol. Evol.*, 18:360, 1982.
- [8] M. Hasegawa, H. Kishino, and T. Yano. Dating of the human-ape splitting by a molecular clock of mitochondrial dna. *J. Mol. Evol.*, 22:160, 1985.
- [9] S. T. Hess, J. D. Blake, and R. D. Blake. Wide variations in neighbor-dependent substitution rates. *J. Mol. Biol.*, 236:1022, 1994.
- [10] S. Karlin and C. . Burge. Dinucleotide relative abundance extremes: a genomic signature. *Trends in Genetics*, 11:283, 1995.
- [11] S. Karlin and J. Mrázek. Compositional differences within and between eukaryotic genomes. *Proc. Natl. Acad. Sci. USA*, 94:10227, 1997.
- [12] S. Karlin, J. Mrázek, and A. M. Campbell. Compositional biases of bacterial genomes and evolutionary implications. *J. Bact.*, 179:775, 1978.
- [13] W. H. Li, C. I. Wu, and C. C. Luo. Nonrandomness of point mutation as reflected in nucleotide substitutions in pseudogenes and its evolutionary implications. *J. Mol. Evol.*, 21:58, 1984.
- [14] J. Neyman. In S. S. Gupta and J. Yackel, editors, *Statistical decision theory and related topics*. Academic Press, New York, 1971.
- [15] D. A. Petrov and D. L. Hartl. Patterns of nucleotide substitution in drosophila and mammalian genomes. *Proc. Natl. Acad. Sci. USA*, 96:1475, 1999.
- [16] A. Razin and A. D. Riggs. Dna methylation and gene function. *Science*, 210:604, 1980.
- [17] G. J. Russell and J. H. Subak-Sharpe. Similarity of the general designs of protochordates and invertebrates. *Nature*, 26:533, 1977.
- [18] G. J. Russell, P. M. Walker, R. A. Elton, and J. H. Subak-Sharpe. Doublet frequency analysis of fractionated vertebrate nuclear dna. *J. Mol. Biol.*, 108:1, 1976.
- [19] S. Schwartz, Z. Zhang, K. A. Frazer, A. Smit, C. Riemer, J. Bouck, R. Gibb, R. Hardison, and W. Miller. Pipmaker—a web server for aligning two genomic dna sequences. *Genome Res.*, 10:577, 2000.
- [20] D. G. Wang et al. Large-scale identification, mapping, and genotyping of single-nucleotide polymorphisms in the humane genome. *Science*, 280:1077, 1998.
- [21] Z. Yang and A. D. Yoder. Estimation of the transition/transversion rate bias and species sampling. *J. Mol. Evol.*, 48:274, 1984.

APPENDIX

A. THE TWO-CLUSTER APPROXIMATION

To illustrate our method, we consider a specific example of the neighbor-dependent mutation process, the CpG-methylation-deamination process mentioned in the introduction. A similar model has also been studied using Monte-Carlo simulations in Ref. [5]. Given the mutation processes defined by Eqs. (6), (7) and (8), the time evolution of the dinucleotide frequency $f_{\alpha\beta}$ can be expressed in terms of the function $f_{\alpha\beta}$ and the trinucleotide frequency $f_{\alpha\beta\gamma}$ only. It will be convenient to take the continuum time limit, and turn the discrete dynamics described in Sec. 2 into differential equations[6]. For example, the evolution of f_{AA} is given by

$$\begin{aligned} \frac{\partial}{\partial t} f_{AA} = & p f_{CA} + q f_{GA} + p f_{TA} - (2p + q) f_{AA} \\ & + p f_{AC} + q f_{AG} + p f_{AT} - (2p + q) f_{AA} + r f_{CGA} \end{aligned} \quad (10)$$

where all terms on the right hand side correspond to processes either creating (positive signs) or destroying (negative signs) an AA pair. In Eq. (10), the first four terms result from point mutations on the first site, the second four from point mutations on the second site, as indicated by the underlined letters. The last term proportional to r stems from a G turning into an A due to a CG \rightarrow CA process on the two sites shifted by one to the left. There are 16 such equations for the 16 dinucleotide frequencies.

As one can see in Eq. (10), the time evolution of the two-point functions depends in general on the three-point functions $f_{\alpha\beta\gamma}$ which in turn will depend on the four-point functions. To truncate this hierarchy of equations, we apply a standard closure approximation used in non-linear dynamics[3]

$$f_{\alpha\beta\gamma} = \frac{f_{\alpha\beta}f_{\beta\gamma}}{f_{\beta}} \quad (11)$$

i.e. we approximate the probability of finding three letters $\alpha\beta\gamma$ by the probability of finding a pair $\alpha\beta$ multiplied by the conditional probability of finding a pair $\beta\gamma$, given that the middle base is β ; the latter is expressed according to Bayes's rule. The L -point function subsequently takes the form

$$f_{\alpha_1 \dots \alpha_L} \approx \prod_{i=2}^L \frac{f_{\alpha_{i-1}\alpha_i}}{f_{\alpha_i}} \quad (12)$$

The single nucleotide frequencies called for in Eqs. (11) and (12) can be expressed in terms of the dinucleotide frequencies as

$$f_{\alpha} = \sum_{\beta} f_{\alpha\beta} = \sum_{\beta} f_{\beta\alpha}. \quad (13)$$

Thus, the right hand side of Eq. (10) can be written as a function of the $f_{\alpha\beta}$'s only. We can generate an equation similar to (10) for each of the 16 $f_{\alpha\beta}$'s. Applying the approximation (11) and the identity (13), we then obtain a closed system of coupled, nonlinear differential equations

$$\frac{\partial}{\partial t} f_{\alpha\beta} = \mathcal{G}_{\alpha\beta}(f_{AA}, f_{AC}, \dots, f_{TT}) \quad (14)$$

with 16 $\mathcal{G}_{\alpha\beta}$'s. In the stationary state, the functions $f_{\alpha\beta}(t)$ are independent of t and hence their derivative with respect to t vanishes. To calculate the stationary $f_{\alpha\beta}$'s, we therefore have to solve the set of 16 (quadratic) equations, $\mathcal{G}_{\alpha\beta}(f_{AA}, f_{AC}, \dots, f_{TT}) = 0$, whose solution is straightforwardly obtained with the help of Mathematica and given below:

It is convenient to express the results in term of the parameter

$$\Delta = \frac{(3p+q)r}{16(p+q)(3p+q) + 4(7p+3q)r}. \quad (15)$$

The single nucleotide frequencies are

$$f_A = f_T = \frac{1}{4} + \frac{\Delta}{2}, \quad f_C = f_G = \frac{1}{4} - \frac{\Delta}{2}. \quad (16)$$

Since Δ is an increasing function of r with $\Delta(r=0) = 0$, we see that $f_A = f_T > 1/4$ for all positive r 's.

The dinucleotide frequencies are most succinctly expressed in terms of the auxiliary functions $\hat{f}_{\alpha\beta} \equiv f_{\alpha\beta} - f_{\alpha}f_{\beta}$. The results are:

$$\hat{f}_{CA} = \frac{\Delta(1+\Delta)}{4}, \quad \hat{f}_{CG} = -\frac{r(1-2\Delta)^2 - 16(p+q)\Delta}{16r} \quad (17)$$

$$\hat{f}_{CC} = -\frac{(2\Delta-1)(4r\Delta^2 + 8(2p+2q+r)\Delta - r)}{32r(\Delta-1)}. \quad (18)$$

Additionally, we have

$$\hat{f}_{AC} = \hat{f}_{AT} = \hat{f}_{CC} = \hat{f}_{CT} = 0 \quad (19)$$

since these four dinucleotides are *two* mutations away from the three primary pairs above, as motivated already in Sec. 3.

The remaining 9 frequencies can now be obtained simply by exploiting the relation $\sum_{\alpha} \hat{f}_{\alpha\beta} = 0 = \sum_{\alpha} \hat{f}_{\beta\alpha}$ which follows from Eq. (13), and the reverse complementarity symmetry $\hat{f}_{\alpha\beta} = \hat{f}_{\bar{\beta}\bar{\alpha}}$. The results are:

$$\hat{f}_{CT} = -(\hat{f}_{CA} + \hat{f}_{CC} + \hat{f}_{CG}), \quad \hat{f}_{TC} = -\hat{f}_{CC}, \quad \hat{f}_{TT} = -\hat{f}_{CT},$$

$$\hat{f}_{AA} = \hat{f}_{TT}, \quad \hat{f}_{AG} = \hat{f}_{CT}, \quad \hat{f}_{GA} = \hat{f}_{TC}, \quad \hat{f}_{GG} = \hat{f}_{CC}, \quad \hat{f}_{TG} = \hat{f}_{CA},$$

$$\hat{f}_{TA} = -(\hat{f}_{AA} + \hat{f}_{CA} + \hat{f}_{GA}).$$

As shown already in Sec. 3, this approximation gives very accurate results when compared to Monte-Carlo simulations of the same system. This is due to the very short-ranged correlation induced by the mutation process and will not be elaborated here.